Cardiovasc Intervent Radiol (2021) 44:1579–1596
https://doi.org/10.1007/s00270-021-02896-0

CLINICAL INVESTIGATION IMAGING

Utility of Real-time CT/MRI-US Automatic Fusion System Based on Vascular Matching in Percutaneous Radiofrequency Ablation for Hepatocellular Carcinomas: A Prospective Study

Seungchul Han[1,2] · Jeong Min Lee[1,2,3] · Dong Ho Lee[1,2] · Jeong Hee Yoon[1,2] · Won Chang[4]

Received: 20 December 2020 / Accepted: 9 June 2021 / Published online: 26 July 2021

Abstract

Purpose To prospectively evaluate the technical success rate of real-time computed tomography/magnetic resonance imaging and ultrasound (CT/MRI-US) automatic fusion system and the long-term therapeutic efficacy of radiofrequency ablation (RFA) guided by automatic fusion in hepatocellular carcinoma (HCC) patients.

Materials and Methods 139 patients with 151 HCCs were prospectively enrolled for RFA guided by an automatic CT/MRI-US fusion system (PercuNav system, Philips, the Netherlands). Automatic fusion imaging, based on vascular segmentation and registration, was performed by sonographic sweeping at the intercostal plane. The fusion quality, tumor localization confidence and technical feasibility were recorded before and after fusion using a scoring system. Technical success rate of the RFA procedure and local tumor progression (LTP) were assessed during follow-up. Analysis of technical success and LTP was performed using generalized estimating equations and Cox proportional hazard regression analysis.

Results The success rate of the fusion system was 82.7% (115/139) per patient. The mean sonographic scan time for fusion was 154.4 ± 108.4 s. In patients with successful fusion, the score indicating tumor localization confidence (2.2 ± 0.8 vs. 2.7 ± 0.9) and technical feasibility (2.6 ± 0.8 vs. 3.4 ± 0.7) increased after fusion ($p < 0.001$). The technical success rate of the RFA procedure was 96.8% (120/124) per tumor in patients with successful fusion, including poorly localized tumors. LTP rates were 8.6%, 12.2% and 15.2% at 1, 2 and 3 years.

Conclusion The CT/MRI-US automatic fusion system showed a high success rate for image registration and facilitated better feasibility and a high technical success rate of RFA in HCCs, even with poor localization on US.

Level of Evidence Level 3b, Nonrandomized prospective study

Keywords Hepatocellular carcinoma · Radiofrequency ablation · CT · MRI-US automatic fusion system

✉ Jeong Min Lee
jmsh@snu.ac.kr

[1] Department of Radiology, Seoul National University Hospital, #101 Daehak-ro, Jongno-gu, Seoul 03080, Republic of Korea

[2] Department of Radiology, Seoul National University College of Medicine, Seoul, Republic of Korea

[3] Institute of Radiation Medicine, Seoul National University Medical Research Center, Seoul, Republic of Korea

[4] Department of Radiology, Seoul National University Bundang Hospital, Seongnam, Republic of Korea

Introduction

Although US guidance can provide real-time guidance in percutaneous ablation procedures, some focal liver lesions may not be seen well because of their isoechogenicity with liver parenchyma or poor sonic window by intervening structures [1, 2]. Several previous studies have reported that CT/MRI-US fusion guidance can mitigate the inherent limitations of each imaging modality, improving the

technical feasibility of ablation procedures as well as local tumor control rates [1, 3–7]. However, registration of two imaging modalities requires expertise and is somewhat time-consuming and suffers from misregistration errors due to different respiration levels as well as the inadequate number of reference anatomical structures in the liver for registration [7–10]. To overcome the limitations of manual registration, automatic registration by liver surface and/or liver vessels between US and MRI or CT has been developed for percutaneous US procedures [8, 11–13]. To date, however, no prospective studies have evaluated the technical success rates of automatic fusion for guiding radiofrequency ablation (RFA) procedures as well as the long-term therapeutic outcomes of RFA guided by automatic CT/MRI-US fusion. Therefore, the purpose of our study was to prospectively evaluate the technical success rate of automatic fusion of real-time CT/MRI-US and the long-term therapeutic efficacy of RFA guided by automatic fusion in patients with hepatocellular carcinoma (HCC).

Materials and Methods

Study Population

A total of 168 patients with 194 malignant liver tumors who were commissioned for RFA at our institution underwent screening for prospective enrollment between August 2015 and November 2016. The inclusion criteria for study enrollment were (1) pathologic or typical imaging-based diagnosis of HCC, (2) multiphase CT or MRI within 3 months ahead of procedure, (3) no evidence of distant metastasis and (4) no contraindications for conventional RFA procedure in our institute, which are uncontrolled coagulopathy (international standard ratio $\geq$ 1.6, or platelet $<$ 50,000//μl), poor cooperation, unfeasible for sedation, portal vein tumor thrombus, tumor number $>$ 4, largest tumor size $>$ 5 cm and tumors abutting portal vein or bile ducts bigger than segmental branches (Appendix 1). Exclusion of patients was done based on the following criteria: (1) the lack of multiphase CT or MRI within 3 months ahead of procedure, (2) RFA planned for palliative purpose, (3) diagnosed as non-HCC malignancy and (4) right hepatectomy state. The preacquired contrast-enhanced liver CT and/or Gd-EOB-DTPA-enhanced MRI and B mode US examination were used for determining tumor size, tumor number and relationship between the tumors and vital structures. After the exclusion of patients according to the exclusion criteria, 139 patients with 151 tumors were finally included for RFA guided by the CT/MRI-US automatic fusion system. Patients who underwent immediate additional transarterial chemoembolization (TACE) after the technical failure of RFA were excluded from the local tumor progression (LTP) analysis (Fig. 1).

For the comparison of the results according to target tumor localization confidence on US, the tumors were classified into one of the three groups: Group A, poorly localized tumors on both B mode US and fusion image; Group B: poorly localized tumors on B mode US, which are well localized after fusion; Group C, well-localized tumors on B mode US and fusion image. ‘Poorly localized’ was defined as a target tumor localization confidence score lower than 3 (invisible or subtle localization). Details of each scoring system are listed in Table 1.

This prospective study was approved by the appropriate institutional review board. Written informed consent was obtained from all subjects before the procedure.

RFA Planning Session

Just before the main RFA procedure, RFA planning US examination was done by an operator (18 years of experience in RFA) with a clinical fellow or a senior resident in the ultrasound suite where the RFA procedure was performed. After planning examination, automatic fusion with US and CT/MRI images was attempted using an ultrasound system (Epiq 5, Philips, Best, the Netherlands) equipped with a 3D fusion software (PercuNav system, Philips, Best, the Netherlands) based on an electromagnetic tracking system that provides the position and orientation of the transducer and patient’s body in the transmitter’s spatial volume [10]. The real-time automatic fusion was achieved by matching the vascular structures in the US image to the correlating structures extracted from the CT or MRI images by auto-segmentation [10]. Automatic fusion was performed by sweeping US scans at the intercostal plane where the main and the right portal vein were observed. US scanning was performed for a maximum of 10 min and 7 times for registration, and failure was considered as inadequate registration after 10 min of attempts. Registration failure was defined as a technical failure due to poor vascular segmentation on US/CT/MRI, or misregistration for both central and peripheral structures $>$ 3 cm. If the automatic fusion failed, manual fusion was performed for the RFA procedure. Repeated assessment of the localization confidence of the tumor, the safety of the approach route, the expected technical feasibility and the expected number of overlapping scans were performed by the operator and the assistant in consensus before and after the fusion process using a scoring system [1]. For the localization of the tumor, additional binomial scale assessment (poorly localized (score 1 and 2) vs. well localized (score 3 and 4)) was done for a more intuitive categorization. The quality of registration after fusion was assessed using a four-point scoring system. The details of the scoring

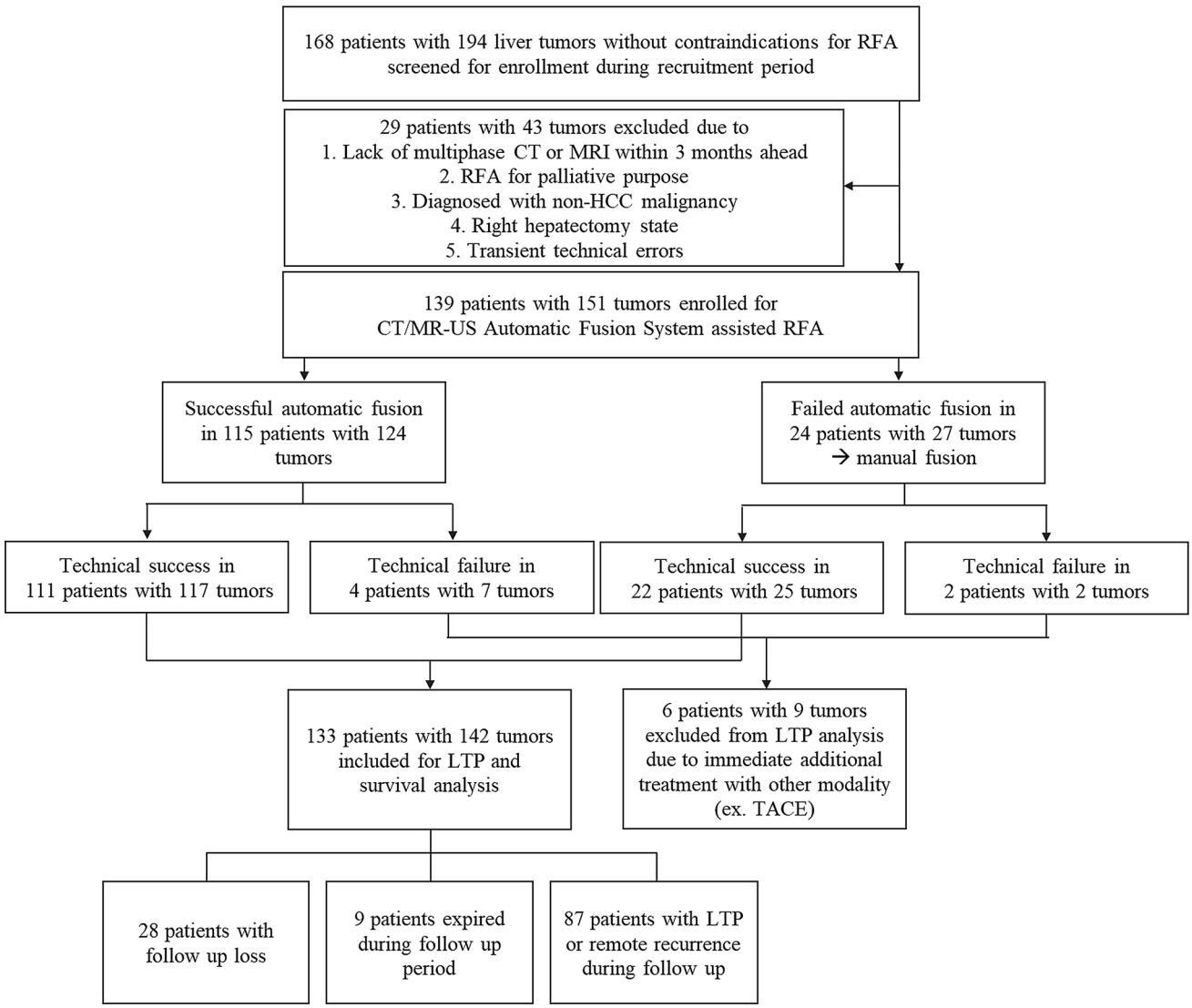

Fig. 1 Flow diagram of patient enrollment

system are provided in Table 1. Technical feasibility was assessed according to the safety of the route and the possibility of complete ablation.

RFA Procedures

The main ablation procedure was conducted by the same senior radiologist assisted by a clinical fellow or a senior resident. A switching monopolar technique with separable clustered electrodes (Octopus electrodes; STARmed, Goyang, Kyunggi, Korea) and a 200 W multichannel generator (VIVA RF System, STARmed) were used for the procedure. The ablation procedure was terminated when the operator expected to achieve complete ablation with a sufficient margin (> 5 mm) on the fusion US image. Immediate post-procedural dynamic CT scan was performed to evaluate the ablation margin and possible complications at the CT unit located next to the RFA unit. Patient underwent contrast-enhanced CT at a 128-row detector scanner (Discovery CT750HD; GE Healthcare, Waukesha, WI, the USA) including precontrast image and arterial- and portal-phase imaging with multiplanar reconstruction (axial, coronal and sagittal) using the low-tube-voltage CT protocol of our institution and the automatic tube-current modulation technique (100 kVp; a noise index of 10.7 HU at 5-mm slice collimations; tube current, variable; detector configuration, 64 × 0.625 mm; beam collimation, 40 mm; and rotation time, 0.5 s). Contrast medium (1.35 mL/kg of Ultravist 370; Bayer Healthcare) was administered intravenously at a rate of 2.0 to 4.0 mL/s using a power injector (Multilevel CT; Medrad, Indianola, PA), followed by a saline flush of approximately 30 to 40 mL. The arterial phase was obtained 19 s after the attenuation of the descending aorta reached 100 HU as

Table 1 Score categories for assessment of target tumor localization confidence, technical feasibility and route safety

Definitions	
*Registration quality**	
1	Failure +
2	Successful for central portion, but misregistration for periphery > 10 mm
3	Successful for both central and peripheral, but misregistration 5 ~ 10 mm
4	Perfect for both central and peripheral, but misregistration < 5 mm
Target tumor localization confidence	
1	Invisible
2	Subtle localization of the tumor by different echogenicities but unclear tumor border
3	Localization with partial delineation of tumor margin
4	Confident localization with clear margin
Technical feasibility	
1	Low
2	Moderate
3	High
4	Highest
Route safety	
1	Bad with segmental branches of PV or HV
2	Adequate with subsegmental small PV, HV branches
3	Safe route with no large vessels

*Registration error was defined as the smallest difference in baseline static position of the liver capsule as well as branching portion of segmental portal vein branch in the tumor-bearing segment when comparing the fused CT/MR dataset and the real-time US images in the same respiratory phase

+ Registration failure was defined a technical failure due to poor vascular segmentation on US/CT/MR, or misregistration for both central and peripheral structures > 3 cm

measured using the bolus tracking method, and the portal venous phase was obtained approximately 70 s after beginning contrast media administration. Technical success was defined, based on the literature, as complete coverage of the tumor by the ablation zone with an ablative margin (> 5 mm) on immediate follow-up [14].

Post-procedural Follow-up

Follow-up contrast-enhanced CT or MRI scans were performed 1 month after the procedure, followed by serial CT or MRI scans at 3-month intervals for the first year and 4–6-month intervals for the second year. Technical efficacy was determined at 1 month after the procedure based on the literature [14]. LTP was assessed during the follow-up period. LTP was defined, based on the literature, as a new tumor focus at the margin of the ablation zone [14].

Statistical Analysis

The normality of distribution was assessed using the Shapiro–Wilk test. The chi-squared or Fisher's exact test was used to determine the significance of the differences in the categorical variables, and the Mann–Whitney U test or Student's *t* test was used to compare continuous variables. The analysis of patients with multiple tumors was performed using generalized estimating equations. Survival analysis and comparison were performed using the Kaplan–Meier analysis and the log-rank test. Risk factors for LTP were evaluated through the Cox proportional hazard regression analysis. All statistical analyses were performed using SPSS software (version 22; SPSS Inc., Chicago, IL, the USA), and $p < 0.05$ was considered statistically significant.

Results

Baseline Characteristics

The baseline characteristics of the enrolled population are summarized in Table 2. The majority of the tumors were de novo (64.2% [97/151]), located at S7/8 (49.0% [74/151]), and smaller than 3 cm in size (90.7% [137/151]). The median interval between the imaging and RFA procedures was 26 days. The median follow-up period was 47.4 months for patients included in LTP and survival analysis (Table 1). Only 1 patient (0.7%) suffered from a major complication (bleeding which required embolization) after the procedure. Regarding subgroups stratified by

Table 2 Baseline characteristics of study population

Baseline characteristics (n = 139 patients, 151 tumors)	
Sex (M: F)	105:34 (75.5:24.5)
Age (year, mean ± SD)	63.5 ± 9.6
BMI (kg/m2)	24.9 ± 3.6
Liver cirrhosis	133/139 (95.7)
Child–Pugh classification (A/B)	135/4
BCLC stage	
Very early (0)	72/139 (51.8)
Early (A)	59/139 (42.4)
Intermediate (B)	8/139 (5.8)
Image modality and dynamic phase used for fusion process	
CT	74/139 (53.2)
Arterial phase	15/74 (20.3)
Portal phase	50/74 (67.6))
Delayed phase	9/74 (12.2)
MR	65/139 (46.8)
Arterial phase	6/65 (9.2)
Portal phase	3/65 (4.6)
Transitional phase	0/65 (0.0)
Hepatobiliary phase	56/65 (86.2)
Median interval between imaging and procedure (days, range)	26 [0–80]
*Tumor location**	
Left lobe (S2, S3, S4)	27/151 (17.9)
Right superior segments (S7, S8)	74/151 (49.0)
Right inferior segments (S5, S6)	50/151 (33.1)
Tumor size (cm, mean ± SD)*	1.9 ± 0.8
< 3 cm	137/151 (90.7)
≥ 3 cm	14/151 (9.3)
*Tumor nature**	
De novo tumor	97/151 (64.2)
Recurred tumor	54/151 (35.8)
Underlying liver disease	
Alcoholic liver disease	8/139 (5.8)
HBV	105/139 (75.5)
HCV	20/139 (14.4)
HBV & HCV	1/139 (0.7)
Non-HBV, HCV	4/139 (2.9)
Primary biliary cirrhosis	1/139 (0.7)
*Previous treatment for HCC**	
RFA	44/151 (29.1)
TACE	85/151 (56.3)
PEIT	19/151 (12.6)
Surgical resection	12/151 (7.9)
Liver transplantation	1/151 (0.7)
Insertion of artificial ascites	89 (64.0)
Major complications**	1/139 (0.7)
Median follow-up period	
(months, range)**	47.4 [1.0–55.0]

Unless indicated, data are number of patients or tumors, with the percentage in parentheses. * Statistics per tumor, otherwise per patient, **Includes vascular or bile duct injury, massive bleeding and pneumothorax. ***For patients included in LTP and survival analysis, BCLC stage = Barcelona clinic liver cancer stage

the localization confidence of target lesions on B mode US and fusion images, there were 62 group A, 41 group B and 48 group C lesions (Appendix 6).

Success rate of Image Registration in the Automatic Fusion Process

The overall success rate of the vascular matching-based CT/MRI-US automatic fusion system in image registration was 82.7% (115/139) per patient. Furthermore, 74.1% (103/139) of the patients showed high-quality registration, which was defined as registration for central and peripheral portions with misregistration of less than 10 mm (Fig. 2). The mean scan duration and number of scans for automatic fusion were 154.4 s and 2.6 times, respectively (Table 3).

Comparison of Parameters Before and After Automatic Fusion in RFA Planning Session

In patients with successful automatic fusion, overall target tumor localization confidence increased after fusion in both the binomial scale (34.7% [43/124] vs. 62.9% [78/124], $p < 0.001$) and localization confidence score (2.2 ± 0.8 vs. 2.7 ± 0.9, $p < 0.001$) compared with the B mode US scans; this was particularly observed in tumors smaller than 3 cm (31.9% [36/113] vs. 61.9% [70/113], $p < 0.001$). The expected technical feasibility significantly increased after automatic fusion (2.6 ± 0.8 vs. 3.4 ± 0.7, $p < 0.001$). There was a significant difference between the expected overlap numbers before and after automatic fusion (1.2 ± 0.5 vs. 1.3 ± 0.6, $p = 0.001$). The rate of change in the approach route after fusion was 78.2% (97/124) (Table 4).

Short-Term Therapeutic Outcome of the Automatic Fusion-Assisted RFA Procedure

All the patients who achieved technical success were confirmed to have complete ablation of the tumor on immediate follow-up and 1-month follow-up CT; therefore, the results on technical success and efficacy were identical. The overall technical success rate per tumor was 96.0% (145/151) for the total enrolled patients and 96.8% (120/124) in patients with successful automatic fusion. In patients with successful automatic fusion, the technical success rate based on technical feasibility was significantly different, and it was the lowest (57.1% [4/7]) when the expected technical feasibility was moderate ($p < 0.001$). The analysis of technical success using the variables is summarized in Appendix 4.

Analysis of Local Tumor Progression

The rate of LTP per tumor at 1, 2 and 3 years in all enrolled patients was 8.6%, 11.6% and 14.9%, respectively. In patients with successful automatic fusion, the incidence of LTP per tumor at 1, 2 and 3 years was 8.6%, 12.2% and 15.2%, respectively (Fig. 3). The analysis for LTP in patients with successful automatic fusion revealed that tumors with low (HR, 45.20 [5.92–344.94]; $p < 0.001$) and high (HR, 3.83 [1.11–13.18]; $p = 0.03$) expected feasibility showed a higher risk of LTP than these with the highest expected feasibility ($p = 0.004$) (Table 5).

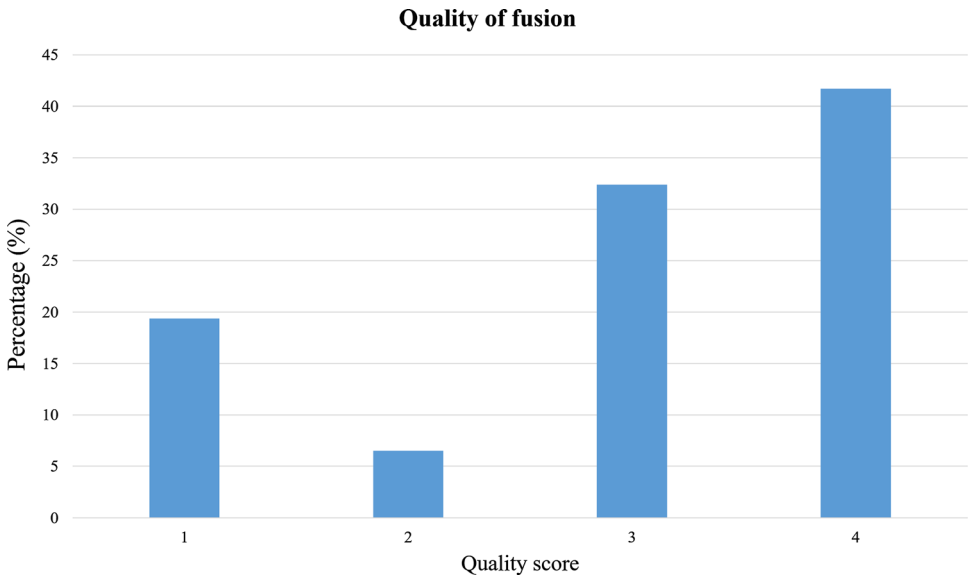

Fig. 2 Quality assessment of automatic CT/MR-US fusion technique. Score categories are as following: 1; failure, 2; successful for central portion, but misregistration for periphery > 10 mm, 3; successful for both central and peripheral, but misregistration 5 ~ 10 mm, 4; perfect for both central and peripheral, but misregistration < 5 mm

Table 3 Automatic fusion success rate and fusion properties

	Results		*P* value
	CT	MR	
Overall success rate	115/139 (82.7)		
Overall fusion quality	3.0 ± 1.1		
Success rate per method	69/74 (93.2)	46/65 (70.8)	0.001
Fusion quality per method	3.2 ± 0.9	2.6 ± 1.3	0.02
Scan time (sec)			
Overall	154.4 ± 108.4		
Per method	151.9 ± 103.1	158.04 ± 117.0	0.96
Scan number			
Overall	2.6 ± 1.6		
Per method	2.6 ± 1.6	2.5 ± 1.7	0.80

Unless indicated, data are number of patients or tumors, with the percentage in parentheses. Ordinary and continuous variables were expressed as mean value with standard deviation. Test for normal distribution was done by Shapiro–Wilk test. Comparison of independent categorical variables was done by Pearson's Chi-square test or Fischer's exact test. Comparison of continuous variables was done by Mann–Whitney U test

Table 4 Results from pre-procedural planning session in patients with successful automatic fusion

	Results (n = 124)		*P* value
Target tumor localization confidence	Conventional US	Automatic CTMR-fusion US	
Total			
Well-localized tumors*	43/124 (34.7)	78/124 (62.9)	< 0.001
Localization confidence score	2.2 ± 0.8	2.7 ± 0.9	< 0.001
By location (binomial)*			
Left lobe	9/21 (42.9)	14/21 (66.7)	0.03
Right superior segments	16/62 (25.8)	31/62 (50.0)	< 0.001
Right inferior segments	20/50 (40.0)	36/50 (72.0)	< 0.001
By location (score)			
Left lobe	2.3 ± 0.9	2.8 ± 0.9	< 0.001
Right superior segments	2.0 ± 0.8	2.4 ± 0.9	< 0.001
Right inferior segments	2.5 ± 0.8	3.1 ± 0.8	< 0.001
By size (binomial)*			
< 3 cm	36/113 (31.9)	70/113 (61.9)	< 0.001
≥ 3 cm	7/11 (63.6)	8/11 (72.7)	0.30
By size (score)			
< 3 cm	2.2 ± 0.8	2.7 ± 0.9	< 0.001
≥ 3 cm	2.7 ± 0.6	2.9 ± 0.7	0.12
Safety route assessment	Conventional US	Automatic CTMR-fusion US	
	2.1 ± 0.7	1.8 ± 0.7	< 0.001
Expected technical feasibility	Conventional US	Automatic CTMR-fusion US	
	2.6 ± 0.8	3.4 ± 0.7	< 0.001
Expected overlaps	Conventional US	Automatic CTMR-fusion US	
	1.2 ± 0.5	1.3 ± 0.6	0.001
Rate of changing route			
		97/124 (78.2)	

Unless indicated, data are number of patients or tumors, with the percentage in parentheses. Ordinary and continuous variables were expressed as mean value with standard deviation. Test for normal distribution was done by Shapiro–Wilk test. Analysis regarding patients with multiple tumors was done using generalized estimating equations. * Binomial scale was categorized as following: Poorly localized (score 1 and 2) vs. well localized (score 3 and 4)

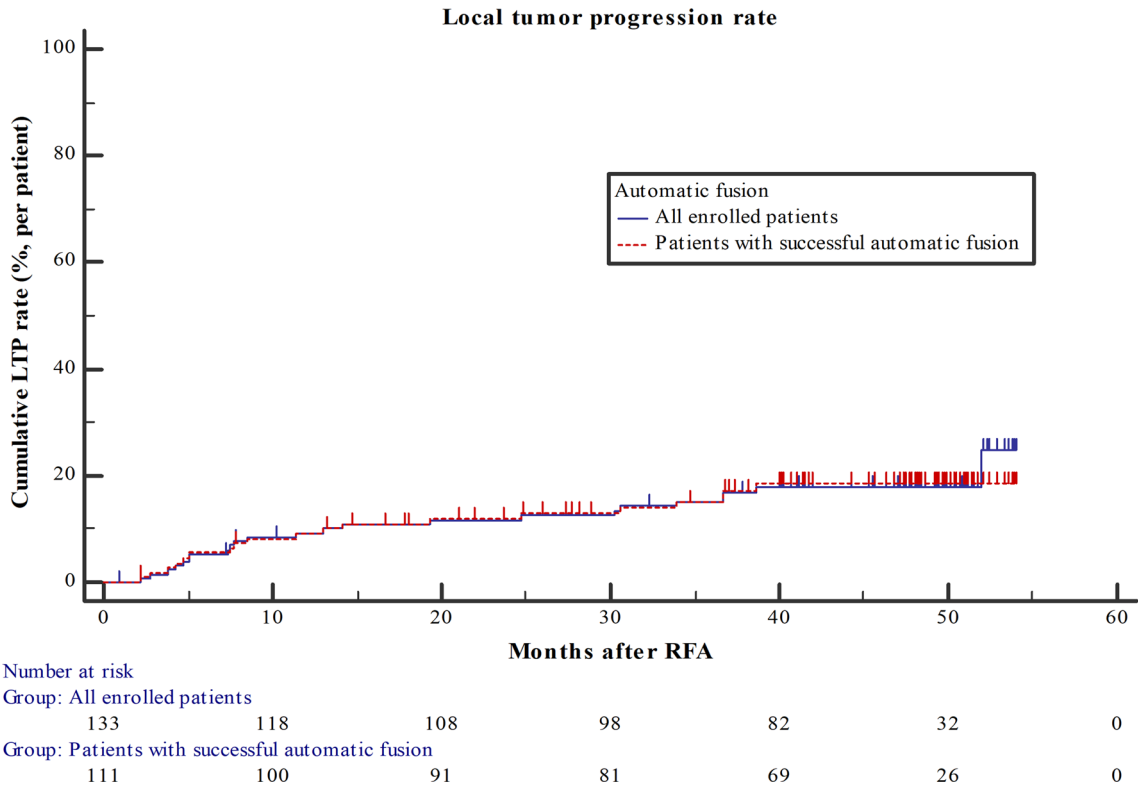

Fig. 3 Cumulative LTP in entire enrolled patients and in patients with successful automatic fusion. Kaplan–Meier curves representing the development of LTP in entire enrolled patients and in patients with successful automatic fusion ($p = 0.98$)

Comparison of Therapeutic Outcomes Between Subgroups of Tumors According to Localization Confidence

The technical success rates of the overall RFA procedure of the three subgroups were not significantly different ($p = 0.22$) (Table 6). However, the incidence of LTP in group A tumors were 14.6%, 22.2% and 27.6% at 1, 2 and 3 years, respectively, which were higher than those of tumors in groups B and C ($p = 0.018$) (Fig. 4).

Discussion

In our study, the overall technical success rate of the CT/MRI-US automatic fusion system based on vascular segmentation was 82.7% (115/139). Target tumor localization confidence and technical feasibility significantly increased after successful automatic fusion ($p < 0.001$). Overall technical efficacy (96.3% [78/81]) of automatic fusion-guided RFA in patients with poorly localized tumors on B mode US was similarly excellent to that in patients with well-localized tumors (97.7% [42/43]) (Appendix 4). The therapeutic outcome of the RFA procedure assisted by the automatic fusion system in our study was similar or even better in several aspects than these reported in the literature, despite the fact that there were many tumors (67.8% [103/152]) with poor conspicuity of HCCs on B mode US which may be excluded from the procedure in practice [1, 5] (Fig. 5). The mean scan duration of automatic fusion (154.4 s) was comparable to those reported by previous studies using manual fusion by experts, and it is practically acceptable when considering the duration required for patient sedation and equipment preparation [15]. Although few previous studies have reported the technical feasibility of the real-time automatic image fusion technique, our study further suggests the long-term outcomes of automatic CT/MRI-US fusion-assisted RFA in a large number of participants. Based on our study results, an automatic CT/MRI-US fusion system may contribute to the clinical adoption of fusion systems for US-guided procedures, including RFA.

The technical and practical advantages of automatic fusion over manual fusion should be further discussed. First, the automatic fusion technique (PercuNav) used in our study was based on the rigid registration of vascular structures extracted by auto-segmentation from CT or MRI images, which may allow more precise registration in the targeted segment at a faster speed [10]. Difference in breathing motion and organ deformation, which can be obstacles in manual fusion techniques with few registration points, can be less pronounced in the automatic fusion with

Table 5 Risk factor analysis for local tumor progression per tumor in patients with successful automatic fusion

	Univariate		Multivariate	
	Exp (β)	*P* value	Exp (β)	*P* value
Sex (M/F)	1.23 [0.41–3.72]	0.71		
Age	1.01 [0.96–1.06]	0.85		
Location		0.09		0.30
Left lobe	2.99 [0.50–17.87]	0.23	1.79 [0.29–11.13]	0.53
Right superior segments	5.04 [1.14–22.16]	0.03	3.11 [0.67–14.35]	0.15
Right inferior segments				
Tumor size (≥ 3 cm)	1.45 [0.33–6.26]	0.62		
Recurred vs De novo tumor	3.14 [1.26–7.82]	0.01	1.57 [0.55–4.49]	0.40
Target tumor localization confidence		0.03		0.85
Group A	3.33 [1.07–10.33]	0.04	1.37 [0.38–4.88]	0.63
Group B	0.88 [0.20–3.93]	0.87	0.98 [0.21–4.47]	0.97
Group C				
Technical feasibility after fusion		< 0.001		0.004
Low	106.79[16.47–692.20]	< 0.001	45.20 [5.92–344.94]	< 0.001
Moderate	4.36 [0.49–39.06]	0.19	3.17 [0.33–30.85]	0.32
High	4.97 [1.60–15.42]	0.01	3.83 [1.11–13.18]	0.03
Highest				
Expected overlaps after fusion	1.94 [0.96–3.93]	0.06		
Route safety assessed after fusion		0.33		
Bad	2.71 [0.59–12.36]	0.20		
Adequate	1.59 [0.33–7.67]	0.56		
Safe				
Changed route after fusion	5.07 [0.68–37.96]	0.11		
Insertion of artificial ascites	1.21 [0.46–3.17]	0.70		

Unless indicated, data are expressed as coefficient (exp (β)) with 95% confidence interval obtained by Cox regression analysis. * Group A—poorly localized tumors on both B mode US and fusion image, Group B—poorly localized tumors in B mode US which are well localized after fusion, Group C—well-localized tumors on both B mode US and fusion image. Poorly localized tumors are defined as tumors with localization confidence score lower than 3 (invisible or subtle localization)

increased number of registration points [8, 9]. Second, the fusion system includes a patient tracker, and therefore, positional change after registration is possible. Third, although several validation studies of real-time fusion of US and CT/MRI in animal and phantoms demonstrated promising results [16, 17], eventual clinical utility remains speculative as only limited human data regarding registration accuracies are available. According to a previous study by Cha et al. [18] which compared two semi-automatic registration techniques, the median registration error of initial autoregistration was 38.8 mm. 74.1% (103/139) of the patients in our study showed high-quality registration with automatic fusion, which was defined as misregistration of less than 10 mm.

In our study, the long-term results of LTP in automatic fusion imaging-guided RFA were almost equal to those reported in the previous literature (3.2–7.9% at 1-year follow-up) [1, 6, 19]. However, the relatively large proportion of poorly localized tumors in our study may reflect that a large proportion of our patients possessed known factors which contribute to poor localization of the tumor such as advanced cirrhosis, tumors in the right liver dome, and recurred tumors from pretreated lesions with RFA or TACE [1, 2, 9, 15] (Appendix 6). In clinical practice, invisible tumors on the US may be treated with nonsurgical local therapeutic options such as transarterial embolization procedures or stereotactic body radiotherapy [20]. Our results of automatic CT/MRI-US fusion-guided RFA were comparable or superior to those of other nonsurgical local therapeutic options [20–24]. Thus, our study results would be promising when considering the fact that we included and successfully treated such patients with poorly localized tumors on US, which may not be feasible in clinical practice.

Table 6 Technical results in subgroups of tumors regarding localization confidence in patients with successful automatic fusion*

	Group A	Group B	Group C	*P* value
Overall technical success/efficacy	42/45 (93.3)	36/36 (100.0)	42/43 (97.7)	0.22
Tumor location				
Left lobe	7/7 (100.0)	5/5 (100.0)	8/9 (88.9)	0.50
Right superior segments	27/30 (90.0)	16/16 (100.0)	16/16 (100.0)	0.19
Right inferior segments	8/8 (100)	15/15 (100.0)	18/18 (100.0)	N/A
Tumor size				
< 3 cm	39/42 (92.9)	35/35 (100.0)	36/36 (100.0)	0.07
≥ 3 cm	3/3 (100)	1/1 (100.0)	6/7 (85.7)	0.73
Tumor nature				
De novo tumor	20/22 (90.9)	23/23 (100.0)	35/36 (96.3)	0.25
Recurred tumor	22/23 (95.7)	13/13 (100.0)	7/7 (100.0)	0.64
Insertion of artificial ascites				
Yes	32/35 (91.4)	21/21 (100.0)	25/26 (96.2)	0.34
No	10/10 (100.0)	15/15 (100.0)	17/17 (100.0)	N/A

Unless indicated, data are number of patients or tumors, with the percentage in parentheses. Analysis regarding patients with multiple tumors was done using generalized estimating equations. *P* values not available with generalized estimating equations were presented by Fischer's exact test.* Group A—poorly localized tumors on both B mode US and fusion image, Group B—poorly localized tumors in B mode US which are well localized after fusion, Group C—well-localized tumors on both B mode US and fusion image. Poorly localized tumors are defined as tumors with localization confidence score lower than 3 (invisible or subtle localization)

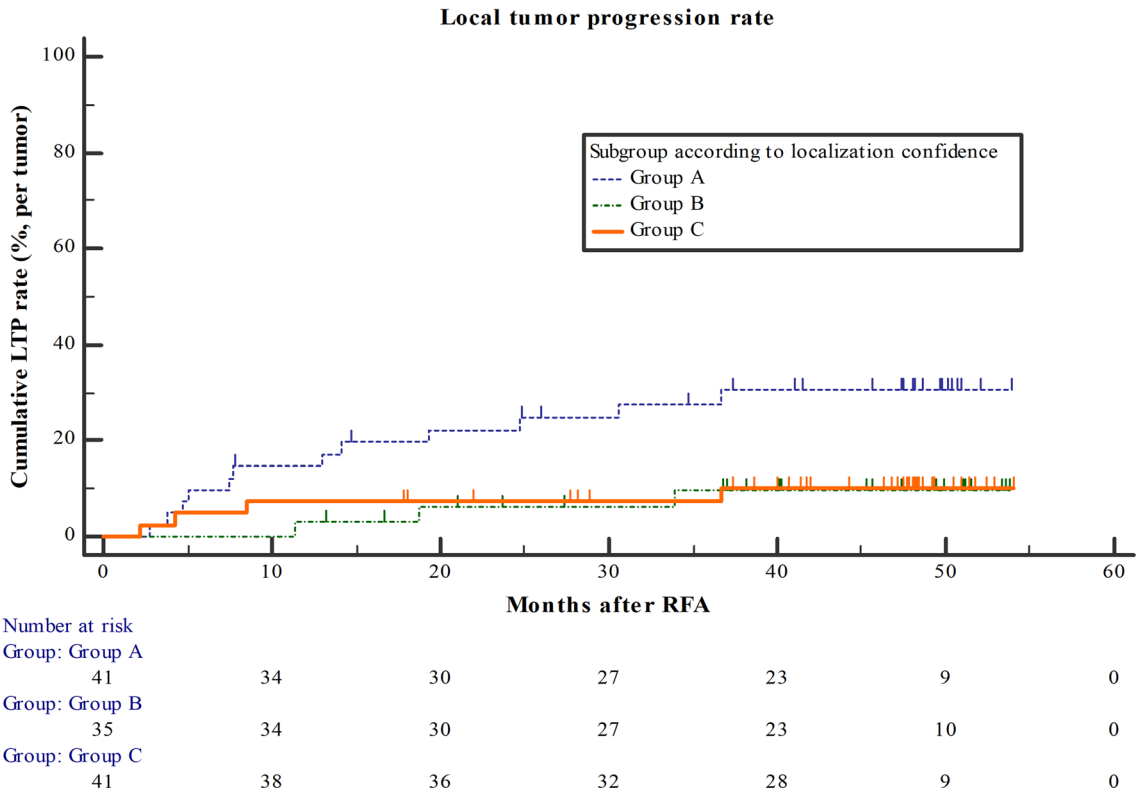

Fig. 4 Cumulative LTP according to target tumor localization confidence in patients with successful automatic fusion. Kaplan–Meier curves representing the development of LTP by subgroup of tumors according to localization confidence in patients with successful automatic fusion ($p = 0.02$)

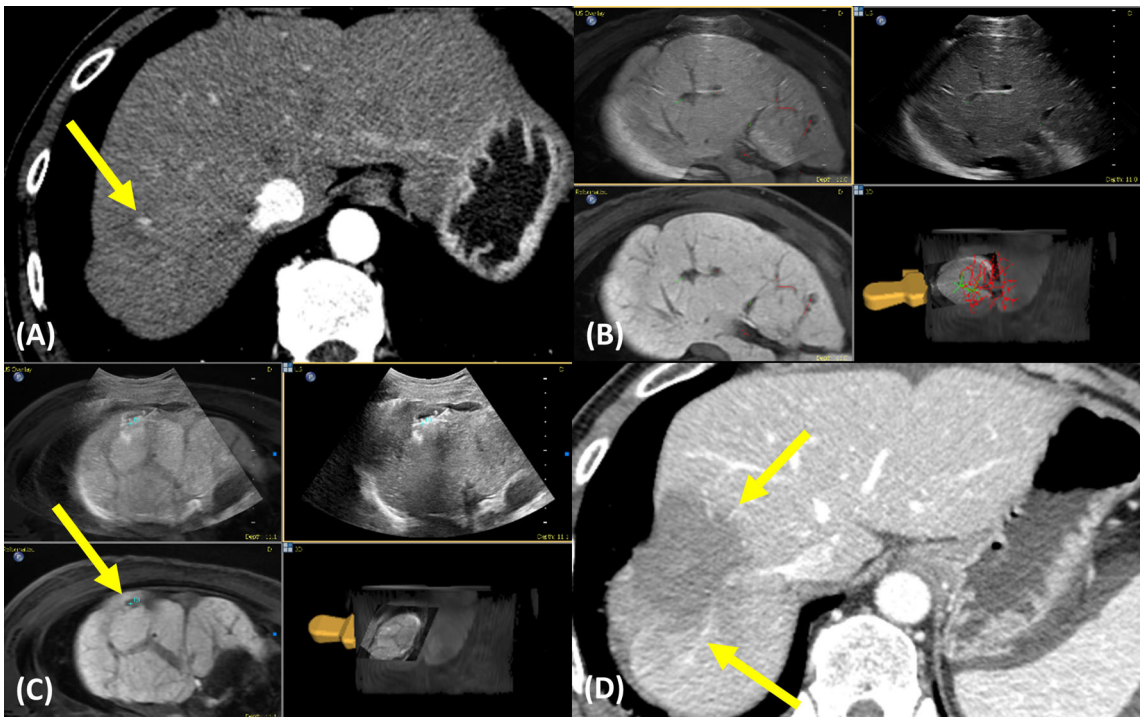

Fig. 5 A representative case of successful automatic fusion followed by complete ablation of the tumor. **A** A 50-year-old man presented with a 0.7 cm-sized recurred HCC at segment 8 liver dome. The initial target tumor localization confidence of the tumor was scored as 'invisible' (score 1) **B** Vascular matching was done, and automatic fusion process was successful. **C** Target tumor localization confidence score increased to 'subtle localization' (score 2) and technical feasibility increased from 'high' (score 3) to 'highest' (score 4) after the fusion process. Automatic CT/MR-US fusion-assisted RFA was done. **D** Successful ablation was confirmed at immediate post-procedural CT scan

Another expected advantage of the automatic fusion is the reduction of major complication rate by increased recognition of vital structures such as portal vein or associated artery and bile ducts in the approach route of the electrodes with precise registration. Our study reported only one major complication (0.7%), which is lower than generally known complication rate in the literature [2, 25, 26]. The reduction of the safety score after fusion, and the high rate of change in approach route in our study may indirectly imply the increased recognition of avoidable structures at the RFA planning session.

This study has several limitations. First, despite the prospective design, our study aimed to be descriptive, and a control group was not used for the comparison of the technical and clinical results. The results were compared to generally known values in the published literature. As this study has suggested the effectiveness and safety of automatic fusion-assisted RFA, further studies including appropriate controls are needed for further validation. Second, the overall RFA procedure was performed primarily by a single experienced radiologist. Therefore, several parameters relied on subjective judgments and the inter-observer variation in the fusion success rate and the procedural outcome was not assessed and the relatively low complication rates require cautious interpretation. However, we may expect similar results with other operators, especially regarding the parameters during the pre-procedural planning, since most of the steps in the image fusion process were automated. Finally, automatic fusion was performed by a single vendor and software from a single manufacturer. Among the two types of automatic fusion that are currently available, only the protocol based on vascular matching was applied; the liver surface-based protocol was left out [8]. Therefore, our results should be interpreted with caution when liver surface-based automatic fusion is applied in clinical practice.

Conclusion

The CT/MRI-US automatic fusion system based on vascular segmentation and matching showed a high success rate of image registration, and it facilitated increased feasibility and high technical success rates of RFA procedures in HCCs, even with poor localization on US.

Acknowledgements This study was conducted under technical support from Philips (Best, the Netherlands) and statistical support from Medical Research Collaborating Center (MRCC) of Seoul National University Hospital

Funding None.

Declarations

Conflict of interest The authors declare that they have no conflict of interest.

Ethical approval All procedures performed in studies involving human participants were in accordance with the ethical standards of the institutional and/or national research committee and with the 1964 Helsinki declaration and its later amendments or comparable ethical standards.

Informed consent Informed consent was obtained from all individual participants included in the study.

Appendix 1

See **Table 7**

Table 7 Contraindications for RFA in our institute

Contraindications for RFA
Coagulopathy (international standard ratio $\geq$ 1.6, or platelet $<$ 50,000/μl)
Poor cooperation
Patient condition is unfeasible for sedation
Portal vein tumor thrombosis
Tumor size $>$ 5 cm
Tumor number $>$ 4
Tumors abutting portal vein or bile ducts bigger than segmental branches

Appendix 2

See **Table 8**

Table 8 Comparison between patients with success and failure in automatic fusion process

	Results		*P* valve
	Success (n = 115)	Failure (n = 24)	
Sex			
M	89/115 (77.4)	16/24 (66.7)	0.27
F	26/115 (22.6)	8/24 (33.3)	
Age (year, mean ± SD)	62.7 ± 9.5	67.7 ± 9.4	0.07
BMI (kg/m^2)			
Non-obese ($<$ 25)	65/115 (56.5)	10/24 (41.7)	0.18
Obese ($\geq$ 25)	50/115 (43.5)	14/24 (58.3)	
Liver cirrhosis	109/115 (94.8)	24/24 (100)	0.59
Fusion modality			
CT	69/115 (60.0)	5/24 (20.8)	0.001
MR	46/115 (40.0)	19/24 (79.2)	
Interval between imaging and procedure (days)*	32 [15–45]	24 [13.25–33.25]	0.11
Underlying liver disease			
Alcoholic liver disease	7/115 (6.1)	1/24 (4.2)	0.30
HBV	86/115 (74.8)	19/24 (79.2)	
HCV	17/115 (14.8)	3/24 (12.5)	
HBV & HCV	1/115 (0.9)	0/24 (0.0)	
Non-HBV, HCV	4/115 (3.5)	0/24 (0.0)	
Primary biliary cirrhosis	0/115 (0.0)	1/24 (4.2)	

Unless indicated, data are number of patients or tumors, with the percentage in parentheses. Ordinary and continuous variables were expressed as mean value with standard deviation or *median with interquartile range. Test for normal distribution was done by Shapiro–Wilk test. Comparison of independent categorical variables was done by Pearson's Chi-square test or Fischer's exact test

Appendix 3

See **Table 9**

Table 9 Results from pre-procedural planning session in entire enrolled patients

	Results		*P* value
Target tumor localization confidence	Conventional US	CTMR-fusion US	
Total			
Well-localized tumors*	57/151 (37.7)	92/151 (60.9)	< 0.001
Localization confidence score	2.2 ± 0.8	2.6 ± 0.9	< 0.001
By location (Number of well-localized tumors, binomial)*			
Left lobe	11/27 (40.7)	17/27 (63.0)	0.017
Right superior segment	17/74 (23.0)	35/74 (47.3)	< 0.001
Right inferior segment	18/41 (43.9)	33/41 (80.5)	< 0.001
By location (Localization confidence score)			
Left lobe	2.3 ± 0.9	2.7 ± 0.9	< 0.001
Right superior segment	2.0 ± 0.7	2.4 ± 0.9	< 0.001
Right inferior segment	2.4 ± 0.9	2.9 ± 0.8	< 0.001
By size (Number of well-localized tumors, binomial)*			
< 3 cm	40/137 (29.2)	77/137 (56.2)	< 0.001
≥ 3 cm	8/14 (57.1)	11/14 (78.6)	0.061
By size (Localization confidence score)			
< 3 cm	2.2 ± 0.8	2.6 ± 0.9	< 0.001
≥ 3 cm	2.6 ± 0.6	2.9 ± 0.6	0.018
Safety route assessment	Conventional US	CTMR-fusion US	
	2.0 ± 0.7	1.8 ± 0.7	< 0.001
Expected technical feasibility	Conventional US	CTMR-fusion US	
	2.6 ± 0.8	3.4 ± 0.7	< 0.001
Expected overlaps	Conventional US	CTMR-fusion US	
	1.3 ± 0.5	1.4 ± 0.6	< 0.001
Rate of changing route			
		118/151 (78.1)	

Unless indicated, data are number of patients or tumors, with the percentage in parentheses. Ordinary and continuous variables were expressed as mean value with standard deviation. Test for normal distribution was done by Shapiro–Wilk test. Analysis regarding patients with multiple tumors was done using generalized estimating equations

*Binomial localization confidence scale was categorized as following: Poorly localized (score 1 and 2) vs. well localized (score 3 and 4)

Appendix 4

See **Table 10**

Table 10 Analysis for technical success/efficacy per tumor

	Results			
	Total enrolled (n = 151)	P value	Successful automatic fusion (n = 124)	P valve
Overall rate	145/151 (96.0)		120/124 (96.8)	
Sex				
M	106/111 (95.5)	0.92	90/93 (96.8)	0.42
F	39/40 (97.5)		30/31 (96.8)	
Age*	0.95 [0.87–1.04]	0.28	0.88 [0.76–1.00]	0.07
BMI (kg/m^2)				
Non-obese (< 25)	77/81 (95.1)	0.36	69/71 (97.2)	0.55
Obese (≥ 25)	68/70 (97.1)		51/53 (96.2)	
Liver cirrhosis	138/144 (95.8)	0.99	114/117 (97.4)	0.99
Location				
Left lobe	24/27 (88.9)	0.45	20/21 (95.2)	0.36
Right superior segments	71/74 (95.9)		59/62 (95.2)	
Right inferior segments	50/50 (100)		41/41 (100)	
Size				
< 3 cm	132/137 (96.4)	0.62	110/113 (97.3)	0.94
≥ 3 cm	13/14 (92.9)		10/11 (90.9)	
Tumor nature				
De novo tumor	94/97 (93.1)	0.30	78/81 (97.5)	0.09
Recurred tumor	51/54 (94.4)		42/43 (97.7)	
Automatic CT/MR-fusion				
Fail	25/27 (92.6)	0.50		
Success	120/124 (96.8)			
*Target tumor localization confidence***				
Group A	58/62 (93.5)	0.26	42/45 (93.3)	0.22
Group B	41/41 (100.0)		36/36 (100.0)	
Group C	46/48 (95.8)		42/43 (97.7)	
Technical feasibility after fusion				
Low	2/2 (100)	< 0.001	2/2 (100)	< 0.001
Moderate	9/14 (64.3)		4/7 (57.1)	
High	60/61 (98.4)		47/48 (97.9)	
Highest	74/74 (100)		67/67 (100)	
Expected overlaps after fusion*	1.11 [0.28–4.49]	0.78	0.67 [0.16–2.77]	0.76
Route safety assessed after fusion				
Bad	58/63 (92.1)	0.08	45/48 (93.8)	0.20
Adequate	61/61 (100)		52/52 (100)	
Safe	26/27 (96.3)		23/24 (95.8)	
Changing route after fusion				
Yes	114/118 (96.6)	0.24	94/97 (93.9)	0.001

Table 10 continued

	Results			
	Total enrolled (n = 151)	P value	Successful automatic fusion (n = 124)	P valve
No	31/33 (93.9)		26/27 (96.3)	
Insertion of artificial ascites				
Yes	94/98 (95.9)	0.74	78/82 (95.1)	0.30
No	51/53 (96.2)		42/42 (100)	

Unless indicated, data are number of patients or tumors, with the percentage in parentheses. Test for normal distribution was done by Shapiro–Wilk test. Analysis regarding patients with multiple tumors was done using generalized estimating equations. P values not available with generalized estimating equations were presented by Pearson's chi square test

*Results of analysis on continuous variables were expressed as coefficient (exp (β)) with 95% confidence interval obtained by binary logistic regression analysis

*** Group A—poorly localized tumors on both B mode US and fusion image, Group B—poorly localized tumors in B mode US which are well localized after fusion, Group C—well-localized tumors on both B mode US and fusion image. Poorly localized tumors are defined as tumors with localization confidence score lower than 3 (invisible or subtle localization)

Appendix 5

See **Table 11**

Table 11 Risk factor analysis for local tumor progression per tumor in entire enrolled patients

	Univariate		Multivariate	
	Exp (β)	P value	Exp (β)	P value
Sex (M/F)	0.97 [0.38–2.48]	0.95		
Age	1.00 [0.96–1.05]	0.86		
Location		0.10		0.30
Left lobe	2.80 [0.63–12.51]	0.09	2.04 [0.43–9.66]	0.37
Right superior segments	3.88 [1.13–13.32]	0.03	2.72 [0.76–9.76]	0.13
Right inferior segments				
Tumor size (≥ 3 cm)	1.18 [0.28–5.03]	0.82		
Recurred vs De novo tumor	2.60 [1.14–5.97]	0.02	1.72 [0.69–4.28]	0.25
Automatic fusion failure	1.01 [0.34–2.97]	0.99		
Target tumor localization confidence *				
Group A	1.99 [0.77–5.19]	0.16		
Group B	0.58 [0.15–2.32]	0.44		
Group C				
Technical feasibility after fusion		< 0.001		0.01
Low	58.56 [10.72–319.98]	< 0.001	26.29 [4.11–168.30]	0.001
Moderate	2.53 [0.52–12.20]	0.14	1.64 [0.30–9.03]	0.57
High	2.35 [0.923–5.982]	0.07	1.87 [0.67–5.22]	0.23
Highest				
Expected overlaps after fusion	1.46 [0.76–2.79]	0.25		
Route safety assessed after fusion				
Bad	3.09 [0.70–13.70]	0.14		
Adequate	1.89 [0.40–8.92]	0.42		
Safe				
Changed route after fusion	2.91 [0.68–12.41]	0.15		
Insertion of artificial ascites	1.31 [0.54–3.18]	0.55		

Unless indicated, data are expressed as coefficient (exp (β)) with 95% confidence interval obtained by Cox regression analysis

*Group A—poorly localized tumors on both B mode US and fusion image, Group B—poorly localized tumors in B mode US which are well localized after fusion, Group C—well-localized tumors on both B mode US and fusion image. Poorly localized tumors are defined as tumors with localization confidence score lower than 3 (invisible or subtle localization)

Appendix 6

See **Table 12**

Table 12 Comparison of baseline characteristics between subgroups of tumors regarding localization confidence*

	Group A (n = 62)	Group B (n = 41)	Group C (n = 48)	P value
Sex				
M	44/62 (71.0)	31/41 (75.6)	36/48 (75.0)	0.93
F	18/62 (29.0)	10/41 (24.4)	12/48 (25.0)	
Age (year, mean ± SD)	62.8 ± 10.0	63.3 ± 11.0	63.6 ± 9.7	0.45
BMI (kg/m^2)				
Non-obese (< 25)	32/62 (51.6)	23/41 (56.1)	26/48 (54.2)	0.74
Obese (≥ 25)	30/62 (48.4)	18/41 (43.9)	22/48 (45.8)	
Liver cirrhosis	61/62 (98.4)	41/41 (100.0)	42/48 (87.5)	0.01
Pre-procedural imaging modality				
CT	32/62 (51.6)	24/41 (58.5)	21/48 (43.8)	0.38
MR	30/62 (48.4)	17/41 (41.5)	27/48 (56.2)	
Tumor location				
Left lobe	10/62 (16.1)	6/41 (14.6)	11/48 (22.9)	0.08
Right superior segments	38/62 (61.3)	19/41 (46.3)	17/48 (35.4)	
Right inferior segments	14/62 (22.6)	16/41 (39.0)	20/48 (41.7)	
Tumor size				
< 3 cm	59/62 (95.2)	38/41 (92.7)	40/48 (83.3)	0.12
≥ 3 cm	3/62 (4.8)	3/41 (7.3)	8/48 (16.7)	
Tumor nature				
De novo tumor	33/62 (53.2)	26/41 (63.4)	38/48 (79.2)	0.03
Recurred tumor	29/62 (46.8)	15/41 (36.6)	10/48 (20.8)	
Automatic CT/MR-fusion				
Fail	17/62 (27.4)	5/41 (12.2)	5/48 (10.4)	0.60
Success	45/62 (72.6)	36/41 (87.8)	43/48 (89.6)	
Technical feasibility after fusion				
Low	1/62 (1.6)	0/41 (0.0)	1/48 (2.1)	< 0.001
Moderate	9/62 (14.5)	2/41 (4.9)	3/48 (6.3)	
High	38/62 (61.3)	10/41 (24.4)	13/48 (27.1)	
Highest	14/62 (22.6)	29/41 (70.7)	31/48 (64.6)	
Expected overlaps after fusion	1.2 ± 0.4	1.5 ± 0.6	1.5 ± 0.8	< 0.001
Route safety assessed after fusion				
Bad	26/62 (41.9)	15/41 (36.6)	22/48 (45.8)	0.73
Adequate	23/62 (37.1)	20/41 (48.8)	18/48 (37.5)	
Safe	13/62 (21.0)	6/41 (14.6)	8/48 (16.7)	
Changing route after fusion				
Yes	51/62 (82.3)	33/41 (80.5)	34/48 (70.8)	0.43
No	11/62 (17.7)	8/41 (19.5)	14/48 (29.2)	
Insertion of artificial ascites				
Yes	43/62 (69.4)	25/41 (61.0)	30/48 (62.5)	0.81
No	19/62 (30.6)	16/41 (39.0)	18/48 (37.5)	

Unless indicated, data are number of patients or tumors, with the percentage in parentheses. Ordinary and continuous variables were expressed as mean value with standard deviation. Analysis regarding patients with multiple tumors was done using generalized estimating equations. P values not available with generalized estimating equations were presented by Fischer's exact test. Scale categories are as following:

*Group A—poorly localized tumors on both B mode US and fusion image, Group B—poorly localized tumors in B mode US which are well localized after fusion, Group C—well-localized tumors on both B mode US and fusion image. Poorly localized tumors are defined as tumors with localization confidence score lower than 3 (invisible or subtle localization)

References

1. Ahn SJ, Lee JM, Lee DH, Lee SM, Yoon JH, Kim YJ, et al. Real-time US-CT/MR fusion imaging for percutaneous radiofrequency ablation of hepatocellular carcinoma. J Hepatol. 2017;66(2):347–54. https://doi.org/10.1016/j.jhep.2016.09.003.
2. Kang J, Ryu JK, Son JH, Lee JW, Choi JH, Lee SH, et al. Association between pathologic grade and multiphase computed tomography enhancement in pancreatic neuroendocrine neoplasm. J Gastroenterol Hepatol. 2018. https://doi.org/10.1111/jgh.14139.
3. Mauri G, Cova L, De Beni S, Ierace T, Tondolo T, Cerri A, et al. Real-time US-CT/MRI image fusion for guidance of thermal ablation of liver tumors undetectable with US: results in 295 cases. Cardiovasc Intervent Radiol. 2015;38(1):143–51. https://doi.org/10.1007/s00270-014-0897-y.
4. Calandri M, Mauri G, Yevich S, Gazzera C, Basile D, Gatti M, et al. Fusion imaging and virtual navigation to guide percutaneous thermal ablation of hepatocellular carcinoma: a review of the literature. Cardiovasc Intervent Radiol. 2019;42(5):639–47. https://doi.org/10.1007/s00270-019-02167-z.
5. Lee MW, Rhim H, Cha DI, Kim YJ, Choi D, Kim YS, et al. Percutaneous radiofrequency ablation of hepatocellular carcinoma: fusion imaging guidance for management of lesions with poor conspicuity at conventional sonography. AJR Am J Roentgenol. 2012;198(6):1438–44. https://doi.org/10.2214/AJR.11.7568.
6. Song KD, Lee MW, Rhim H, Kang TW, Cha DI, Sinn DH, et al. Percutaneous US/MRI fusion-guided radiofrequency ablation for recurrent subcentimeter hepatocellular carcinoma: technical feasibility and therapeutic outcomes. Radiology. 2018;288(3):878–86. https://doi.org/10.1148/radiol.2018172743.
7. Xu ZF, Xie XY, Kuang M, Liu GJ, Chen LD, Zheng YL, et al. Percutaneous radiofrequency ablation of malignant liver tumors with ultrasound and CT fusion imaging guidance. J Clin Ultrasound. 2014;42(6):321–30. https://doi.org/10.1002/jcu.22141.
8. Kim AY, Lee MW, Cha DI, Lim HK, Oh YT, Jeong JY, et al. Automatic registration between real-time ultrasonography and pre-procedural magnetic resonance images: a prospective comparison between two registration methods by liver surface and vessel and by liver surface only. Ultrasound Med Biol. 2016;42(7):1627–36. https://doi.org/10.1016/j.ultrasmedbio.2016.02.008.
9. Lee MW, Park HJ, Kang TW, Ryu J, Bang WC, Lee B, et al. Image fusion of real-time ultrasonography with computed tomography: factors affecting the registration error and motion of focal hepatic lesions. Ultrasound Med Biol. 2017;43(9):2024–32. https://doi.org/10.1016/j.ultrasmedbio.2017.01.027.
10. Ewertsen C, Saftoiu A, Gruionu LG, Karstrup S, Nielsen MB. Real-time image fusion involving diagnostic ultrasound. AJR Am J Roentgenol. 2013;200(3):W249-55. https://doi.org/10.2214/AJR.12.8904.
11. Nam WH, Kang DG, Lee D, Lee JY, Ra JB. Automatic registration between 3D intra-operative ultrasound and pre-operative CT images of the liver based on robust edge matching. Phys Med Biol. 2012;57(1):69–91. https://doi.org/10.1088/0031-9155/57/1/69.
12. Penney GP, Blackall JM, Hamady MS, Sabharwal T, Adam A, Hawkes DJ. Registration of freehand 3D ultrasound and magnetic resonance liver images. Med Image Anal. 2004;8(1):81–91. https://doi.org/10.1016/j.media.2003.07.003.
13. Wein W, Brunke S, Khamene A, Callstrom MR, Navab N. Automatic CT-ultrasound registration for diagnostic imaging and image-guided intervention. Med Image Anal. 2008;12(5):577–85. https://doi.org/10.1016/j.media.2008.06.006.
14. Ahmed M, Solbiati L, Brace CL, Breen DJ, Callstrom MR, Charboneau JW, et al. Image-guided tumor ablation: standardization of terminology and reporting criteria–a 10-year update. J Vasc Interv Radiol. 2014;25(11):1691-705.e4. https://doi.org/10.1016/j.jvir.2014.08.027.
15. Ahn SJ, Lee JM, Chang W, Lee SM, Kang HJ, Yang HK, et al. Clinical utility of real-time ultrasound-multimodality fusion guidance for percutaneous biopsy of focal liver lesions. Eur J Radiol. 2018;103:76–83. https://doi.org/10.1016/j.ejrad.2018.04.002.
16. Appelbaum L, Solbiati L, Sosna J, Nissenbaum Y, Greenbaum N, Goldberg SN. Evaluation of an electromagnetic image-fusion navigation system for biopsy of small lesions: assessment of accuracy in an in vivo swine model. Acad Radiol. 2013;20(2):209–17. https://doi.org/10.1016/j.acra.2012.09.020.
17. Krucker J, Xu S, Glossop N, Viswanathan A, Borgert J, Schulz H, et al. Electromagnetic tracking for thermal ablation and biopsy guidance: clinical evaluation of spatial accuracy. J Vasc Interv Radiol. 2007;18(9):1141–50. https://doi.org/10.1016/j.jvir.2007.06.014.
18. Cha DI, Lee MW, Kim AY, Kang TW, Oh YT, Jeong JY, et al. Automatic image fusion of real-time ultrasound with computed tomography images: a prospective comparison between two auto-registration methods. Acta Radiol. 2017;58(11):1349–57. https://doi.org/10.1177/0284185117693459.
19. Yoon JH, Lee JM, Klotz E, Woo H, Yu MH, Joo I, et al. Prediction of local tumor progression after radiofrequency ablation (RFA) of hepatocellular carcinoma by assessment of ablative margin using Pre-RFA MRI and Post-RFA CT registration. Korean J Radiol. 2018;19(6):1053–65. https://doi.org/10.3348/kjr.2018.19.6.1053.
20. Au KP, Chiang CL, Chan ACY, Cheung TT, Lo CM, Chok KSH. Initial experience with stereotactic body radiotherapy for intrahepatic hepatocellular carcinoma recurrence after liver transplantation. World J Clin Cases. 2020;8(13):2758–68. https://doi.org/10.12998/wjcc.v8.i13.2758.
21. Baek MY, Yoo JJ, Jeong SW, Jang JY, Kim YK, Jeong SO, et al. Clinical outcomes of patients with a single hepatocellular carcinoma less than 5 cm treated with transarterial chemoembolization. Korean J Intern Med. 2019;34(6):1223–32. https://doi.org/10.3904/kjim.2018.058.
22. Iwazawa J, Ohue S, Hashimoto N, Mitani T. Local tumor progression following lipiodol-based targeted chemoembolization of hepatocellular carcinoma: a retrospective comparison of miriplatin and epirubicin. Cancer Manag Res. 2012;4:113–9. https://doi.org/10.2147/cmar.S30431.
23. Zheng L, Li HL, Guo CY, Luo SX. Comparison of the efficacy and prognostic factors of transarterial chemoembolization plus microwave ablation versus transarterial chemoembolization alone in patients with a large solitary or multinodular hepatocellular carcinomas. Korean J Radiol. 2018;19(2):237–46. https://doi.org/10.3348/kjr.2018.19.2.237.
24. Wigg AJ, Narayana SK, Le H, Iankov I, Chinnaratha MA, Tse E, et al. Stereotactic body radiation therapy for early hepatocellular carcinoma: a retrospective analysis of the South Australian experience. ANZ J Surg. 2019;89(9):1138–43. https://doi.org/10.1111/ans.15130.

25. Kong WT, Zhang WW, Qiu YD, Zhou T, Qiu JL, Zhang W, et al. Major complications after radiofrequency ablation for liver tumors: analysis of 255 patients. World J Gastroenterol. 2009;15(21):2651–6. https://doi.org/10.3748/wjg.15.2651.
26. Schullian P, Johnston E, Laimer G, Putzer D, Eberle G, Amann A, et al. Frequency and risk factors for major complications after stereotactic radiofrequency ablation of liver tumors in 1235 ablation sessions: a 15-year experience. Eur Radiol. 2020. https://doi.org/10.1007/s00330-020-07409-0.